JVI Journals.ASM.org

Shift in Monocyte Apoptosis with Increasing Viral Load and Change in Apoptosis-Related ISG/Bcl2 Family Gene Expression in Chronically HIV-1-Infected Subjects

Sean C. Patro,[a,b] Sharmistha Pal,[c] Yingtao Bi,[c] Kenneth Lynn,[d] Karam C. Mounzer,[e] Jay R. Kostman,[d] Ramana V. Davuluri,[c] Luis J. Montaner[a]

The Wistar Institute, HIV Immunopathogenesis Laboratory, Philadelphia, Pennsylvania, USA[a]; University of Pennsylvania Perelman School of Medicine, Department of Microbiology, Philadelphia, Pennsylvania, USA[b]; The Wistar Institute, Center for Systems and Computational Biology, Philadelphia, Pennsylvania, USA[c]; UPENN-Presbyterian Medical Center, Philadelphia, Pennsylvania, USA[d]; Philadelphia FIGHT, The Jonathan Lax Treatment Center, Philadelphia, Pennsylvania, USA[e]

ABSTRACT

Although monocytes and macrophages are targets of HIV-1-mediated immunopathology, the impact of high viremia on activation-induced monocyte apoptosis relative to monocyte and macrophage activation changes remains undetermined. In this study, we determined constitutive and oxidative stress-induced monocyte apoptosis in uninfected and HIV$^+$ individuals across a spectrum of viral loads ($n = 35$; range, 2,243 to 1,355,998 HIV-1 RNA copies/ml) and CD4 counts (range, 26 to 801 cells/mm^3). Both constitutive apoptosis and oxidative stress-induced apoptosis were positively associated with viral load and negatively associated with CD4, with an elevation in apoptosis occurring in patients with more than 40,000 (4.6 log) copies/ml. As expected, expression of Rb1 and interferon-stimulated genes (ISGs), plasma soluble CD163 (sCD163) concentration, and the proportion of CD14^{++} CD16$^+$ intermediate monocytes were elevated in viremic patients compared to those in uninfected controls. Although CD14^{++} CD16$^+$ frequencies, sCD14, sCD163, and most ISG expression were not directly associated with a change in apoptosis, sCD14 and ISG expression showed an association with increasing viral load. Multivariable analysis of clinical values and monocyte gene expression identified changes in IFI27, IFITM2, Rb1, and Bcl2 expression as determinants of constitutive apoptosis ($P = 3.77 \times 10^{-5}$; adjusted $R^2 = 0.5983$), while changes in viral load, IFITM2, Rb1, and Bax expression were determinants of oxidative stress-induced apoptosis ($P = 5.59 \times 10^{-5}$; adjusted $R^2 = 0.5996$). Our data demonstrate differential activation states in monocytes between levels of viremia in association with differences in apoptosis that may contribute to greater monocyte turnover with high viremia.

IMPORTANCE

This study characterized differential monocyte activation, apoptosis, and apoptosis-related gene expression in low- versus high-level viremic HIV-1 patients, suggesting a shift in apoptosis regulation that may be associated with disease state. Using single and multivariable analysis of monocyte activation parameters and gene expression, we supported the hypothesis that monocyte apoptosis in HIV disease is a reflection of viremia and activation state with contributions from gene expression changes within the ISG and Bcl2 gene families. Understanding monocyte apoptosis response may inform HIV immunopathogenesis, retention of infected macrophages, and monocyte turnover in low- or high-viral-load states.

Human immunodeficiency virus type 1 (HIV-1) infection targets CD4-positive T cells, macrophages, and other myeloid cells using CD4 and a chemokine coreceptor (CCR5/CXCR4) (1). While CD4 T-cell loss is observed in tissue (2) and peripheral blood (3, 4) during disease, loss of monocytes and macrophages is less evident. However, monocyte activation, reflected in Toll-like receptor (TLR)-mediated and interferon-stimulated gene (ISG) expression (5–9), monocyte subsets (10–12), and soluble markers of activation (plasma soluble CD14 [sCD14] and CD163 [sCD163]) (12–17), has been described for both early and advanced HIV-1 disease. The impact of HIV-1 viremia on monocyte activation, gene expression (8, 18–20), and function (9–11, 13, 21, 22) is largely independent of productive monocyte infection, as only an estimated 0.03 to 0.1% of circulating monocytes harbor integrated HIV-1 DNA (11, 23, 24). However, exposure to viral particles and proteins, microbial products, and host products (such as cytokines) can modulate monocyte function (8, 19, 20, 25–28) and apoptosis (18, 29–31) during disease.

Unlike for CD4 T cells, the apoptotic fate of monocytes during chronic and elevated HIV and simian immunodeficiency virus (SIV) viremia is less clear, as different *ex vivo* and *in vitro* studies have reported both antiapoptotic (18, 31–33) and proapoptotic (30, 34, 35) mechanisms and outcomes. Gene expression studies have identified a predominant antiapoptosis gene signature in monocytes during chronic disease (18), and

Received 8 August 2014 **Accepted** 21 October 2014

Accepted manuscript posted online 29 October 2014

Citation Patro SC, Pal S, Bi Y, Lynn K, Mounzer KC, Kostman JR, Davuluri RV, Montaner LJ. 2015. Shift in monocyte apoptosis with increasing viral load and change in apoptosis-related ISG/Bcl2 family gene expression in chronically HIV-1-infected subjects. J Virol 89:799–810. doi:10.1128/JVI.02382-14.

Editor: G. Silvestri

Address correspondence Luis J. Montaner, Montaner@wistar.org.

Supplemental material for this article may be found at http://dx.doi.org/10.1128/JVI.02382-14.

doi:10.1128/JVI.02382-14

multiple studies have described antiapoptosis mechanisms *ex vivo* and *in vitro*, including engagement of CCR5 and prosurvival signaling (p38/extracellular signal-regulated kinase/mitogen-activated protein kinase [p38/ERK/MAPK] pathway expression) (18), elevated intracellular zinc content, metallothionein expression (32), elevated Rb1 protein activity (33), and macrophage colony-stimulating factor (M-CSF)-mediated protection from TRAIL-induced apoptosis (31). Based on oxidative stress (36) and increased expression of apoptotic ligands (37–39) in HIV-1 disease, resistance to apoptosis has been tested by multiple induction mechanisms ($CdCl_2$ and sFasL) in cross-sectional studies (18, 31–33). In contrast, nonhuman primate SIV studies have focused on longitudinal changes from early to late disease in highly viremic settings and show higher monocyte turnover and elevated activation markers in animals with rapid disease progression and neuropathogenesis (12, 40, 41), suggesting a functional shift in monocyte viability upon the onset of advanced disease. Other SIV and *in vitro* HIV-1 studies have demonstrated proapoptotic outcomes of viral exposure based on modulation of Bcl2 family genes (Bax, Bak, and Mcl-1), downregulation of antiapoptotic cFLIP proteins, and downregulation of TRAIL decoy receptors (30, 34). While the impact of rising viremia on monocyte activation has been characterized, no HIV-1 study to date has measured macrophage activation with concurrent measurements of monocyte apoptosis to identify functional changes relative to one another and viral load. In addition, studies of antiapoptotic responses in monocytes examined a limited range of viral loads (median viral loads, 14,822 copies/ml [18] and 13,468 copies/ml [33]), thus requiring a more extensive analysis across a wider viral load distribution.

In this study, we reconciled data between independent reports of pro- and antiapoptotic gene expression and functional apoptosis outcomes by the *ex vivo* characterization of circulating monocytes from a broad clinical spectrum of HIV-1 viremia in the absence of antiretroviral therapy (ART).

MATERIALS AND METHODS

Donor population. HIV-1-seropositive patients ($n = 35$; 11.4% female; median age = 43.0 years) were recruited from the Hospital of the University of Philadelphia (HUP) and Philadelphia Field Initiating Group for HIV-1 Trials (FIGHT) and were not on therapy at the time of the single draw. Viremic patients showed a broad spectrum of viremia (viral load range, 2,243 to 1,359,041 copies/ml; CD4 range, 7 to 801 cells/mm^3) (Table 1). Viral load and CD4 count are reported from the most recent clinical visit (at most 3 months). HIV-1-seronegative donors ($n = 33$; 24.2% female; median age, 43.5 years) were recruited from the University of Pennsylvania Human Immunology Core and the Wistar Donors Program (see Table S1 in the supplemental material). Assays data showing less than the total recruited HIV$^-$ or HIV$^+$ population reflect limited patient material. All participants provided informed consent prior to blood draw, and all protocols were approved by the institutional review boards of the National Institutes of Health and The Wistar Institute.

Monocyte and CD4 T-cell isolation and immunophenotyping. Heparinized blood (70 to 200 ml) was processed within 1 to 3 h of draw. Peripheral blood mononuclear cells (PBMC) and plasma samples were obtained using Ficoll-Paque (Amersham Pharmacia Biotech) gradient separation. HIV$^-$ and HIV$^+$ donor CD4 T cells were obtained from the University of Pennsylvania's Center for AIDS Research Human Immunology Core and were collected by Rosette Sep (Stemcell Technologies) isolation from leukapheresis-obtained PBMC product. Monocytes were isolated by negative selection using the Monocyte Isolation Kit II (Miltenyi Biotec; catalog no. 139-091-153) with a mean biological purity greater than 85%. PBMC and isolated monocytes from each sample were stained with CD4-V450, CD14-allophycocyanin (APC), CD16-APCH7, CD3-peridinin chlorophyll protein (PerCP) Cy5.5, and CD8-fluorescein isothiocyanate (FITC) for determination of purity, T-cell subsets, and monocyte subsets. All flow cytometry antibodies were purchased from BD Biosciences and used per the manufacturer's instructions.

TABLE 1 HIV-1 patient population[a]

ID no.	Gender	Age (yr)	Log viral load (copies/ml)	CD4 count (cells/mm^3)
1	M	46	5.44	26
3	M	23	4.97	773
4	M	44	3.35	801
5	M	33	5.67	380
7	M	48	3.72	209
8	M	33	4.38	428
9	M	52	4.93	497
10	M	37	3.97	620
11	M	40	6.13	61
12	M	41	4.56	425
13	M	54	3.96	483
14	M	56	5.64	27
15	M	40	5.49	264
16	M	27	5.18	202
17	M	49	4.31	289
18	M	24	4.18	653
19	M	27	5.54	99
20	M	43	4.61	329
22	M	56	4.59	293
23	M	24	4.85	464
24	M	22	4.15	370
25	M	60	5.45	107
26	M	30	4.64	605
27	F	52	4.41	142
28	M	47	5.00	333
29	M	52	5.07	133
30	F	49	4.58	309
31	M	45	4.61	163
32	F	47	5.29	101
33	M	36	4.64	617
34	M	28	4.62	515
35	M	27	4.10	325
36	M	24	5.04	225
37	F	84	4.29	190
40	M	44	5.76	186
Median		44	4.64	309
IQR		30–49	4.31–5.29	163–464

[a] ID, identification; M, male; F, female; IQR, interquartile range.

Plasma activation markers. HIV$^-$ and HIV$^+$ plasma samples were assayed for sCD14 (R&D Systems) and sCD163 (Trillium Diagnostics), using 1:500 dilutions, according to the manufacturers' instructions. Plates were read on a BioTek Synergy HT microplate reader at 450 nm with the appropriate wavelength corrections.

Quantitative real-time PCR. Total RNA was isolated from 2 million to 5 million cells using the RNeasy Plus II kit (Qiagen) per the manufacturer's protocol. Up to 250 ng of RNA was used with the iScript cDNA synthesis kit (Bio-Rad) as instructed. Quantitative real-time PCR was performed in a 20-μl reaction mixture using Power SYBR green PCR master mix (Life Technologies) and custom-designed primers (Integrated DNA Technologies) (Table 2) using the AB 7000 sequence detection system. The QuantumRNA universal 18S internal standard (Ambion) was used due to its robust and consistent expres-

sion across all samples. All primer sets were assayed by serial dilution PCR across multiple donors to allow for absolute RNA quantification by the standard curve method. The mean of three replicates of each primer-sample pair was used as input in the standard curve method and normalized to the sample's 18S value to generate an absolute RNA expression unit value. (Expression units are defined as expression value relative to 18S after standardization.)

Apoptosis induction assay. Purified monocytes and CD4 T cells were incubated overnight (18 to 22 h) under nonadherent conditions (monocytes in Teflon pots to prevent attachment) in the presence of RPMI 1680 medium with 1% penicillin-streptomycin (Corning), 1% L-glutamine (Corning), and 10% human serum (Gemini Bio-Products) with or without the addition of 20 μM $CdCl_2$ (Sigma). All staining was performed at room temperature (22°C). Between 500,000 and 1 million cells were washed and incubated with flow cytometry wash buffer (Dulbecco's phosphate-buffered saline [Life Technologies] containing 3 mM NaN_3 [Fisher], 1% bovine serum albumin [Sigma], and 5% human serum [Gemini Bio-Products]) as an Fc receptor block. Cells were stained with CD3-Pacific blue, CD14-APC, and 7-aminoactinomycin D (7-AAD) for 15 min. Cell fixation and permeabilization were performed using the BD Cytofix/Cytoperm kit per the manufacturer's instructions and washed in 1× PermWash buffer. Cells were then stained with anti-active caspase 3-phycoerythrin (PE) (BD Biosciences), washed, and resuspended in 300 μl of 1× PermWash buffer. Apoptosis was also assayed at baseline isolation in selected samples. Up to 100,000 events were analyzed on a 14-color LSR II (BD Biosciences).

Gating strategy. Flow cytometry data analysis was performed with FlowJo software (TreeStar) (see Fig. S1 in the supplemental material). Singlets were gated using forward scatter height and area. Live cells were gated, excluding debris and aggregates, with forward and side scatter. To characterize monocyte subsets in PBMC, monocytes were gated based on distinct forward and side scatter parameters and then $CD14^+$ or $CD16^+$ cells within this population. Monocytes were then divided into classical ($CD14^{++}$ $CD16^-$), intermediate ($CD14^{++}$ $CD16^+$), and nonclassical ($CD14^+$ $CD16^{++}$) subsets. In the apoptosis analysis, all events were gated on singlets, intact cells, and either lymphocyte or monocyte forward and side scatter parameters. Cells were analyzed using 7-AAD and caspase-3, and all cells in the early apoptotic and late apoptotic quadrants were counted when determining the percentage of apoptotic cells within the population.

Statistical analysis. All dot, box-and-whisker, and scatter plots were constructed and statistically tested using Prism 4 (GraphPad, La Jolla, CA). All groupwise comparisons were performed using the Mann-Whitney test with *P* value displayed. Correlations between two variables were performed using Spearman's correlation (rho) test with *P* and rho (noted as *R*) values displayed. All tests were two-sided, and a *P* value of <0.05 was considered significant. The Spearman correlation matrix was created with JMP10 software. Based on the analysis of the primary variable (monocyte apoptosis), HIV^+ patient measured variables are presented below and above a viral load cutoff of 40,000 copies/ml ($\log_{10}$ 4.60).

Multivariate linear regression modeling. A stepwise multiple linear regression analysis was performed to model constitutive and induced apoptosis using the combination of clinical and gene expression variables. We conducted log transformation on the independent variables and confirmed lack of multicolinearity in the final models within independent variables by means of the variance inflation factor (VIF). Cook's distance was used in outlier detection and removal of each independent model. The model selection package "leaps" (http://cran.r-project.org/web/packages/leaps/index.html) in R was utilized to identify the best subset of clinical and gene expression parameters that predicted constitutive and induced apoptosis in the linear regression. The regsubsets function within "leaps" was used to find the best subset of predictive parameters. The adjusted *R*-squared statistic was used as the criterion for selecting the best model with four or less variables per total input variable size. Various diagnostic plots were used to check the assumptions for the multiple lin-

TABLE 2 Apoptosis-related p53, Bcl2/cytochrome *c*, and ISG family genes measured by absolute quantitative RT-PCR

Gene designation	Apoptotic impact	Forward primer sequence (5′–3′)	Reverse primer sequence (5′–3′)	Median gene expression (IQR), expression units		*P* value, HIV^- vs HIV^+
				HIV^-, $n = 19$	HIV^+, $n = 30$	
Rb1	Antiapoptotic (22, 27, 61)	GCC TCT CGT CAG GCT TGA G	TCA TCT AGG TCA ACT CGT GCA A	2.559 (1.729–8.421)	7.563 (5.633–9.302)	0.0100
MDM2		GAA TCA TCG GAC TCA GGT ACA TC	TCT GTC TCA CTA ATT GCT CTC CT	1.359 (0.7060–3.316)	1.634 (1.192–2.660)	NS[a]
Bcl2	Antiapoptotic (14, 46, 69)	TTG CCA GCC GGA ACC TAT G	CGA AGG CGA CCA GCA ATG ATA	0.1108 (0.08957–0.3244)	0.3394 (0.09620–0.7771)	NS
Bcl-w	Antiapoptotic (14, 46, 69)	GCG GAG TTC ACA GCT CTA TAC	AAA AGG CCC CTA CAG TTA CCA	1.052 (0.6412–1.314)	0.6553 (0.4295–0.9256)	0.0169
Mcl-1	Antiapoptotic (14, 46, 69)	TGC TTC GGA AAC TGG ACA TCA	TAG CCA CAA AGG CAC CAA AAG	0.8846 (0.5637–1.242)	0.8340 (0.5756–1.101)	NS
Bax	Antiapoptotic (14, 46, 69)	CCC GAG AGG TCT TTT TCC GAG	CCA GCC CAT GAT GGT TCT GAT	0.6709 (0.4939–1.030)	0.8039 (0.6534–0.9233)	NS
Bakl	Antiapoptotic (14, 46, 69)	GTT TTC CGC AGC TAC GTT TTT	GCA GAG GTA AGG TGA CCA TCT C	1.868 (1.338–3.304)	2.201 (1.759–2.906)	NS
Bik	Antiapoptotic (14, 46, 69)	GAC CTG GAC CCT ATG GAG GAC	CCT CAG TCT GGT CGT AGA TGA	0.6191 (0.3536–1.256)	0.6983 (0.4991–1.149)	NS
CycS	Proapoptotic (33, 47)	CTT TGG GCG GAA GAC AGG TC	TTA TTG GCG GCT GTG TAA GAG	0.8745 (0.4069–1.406)	1.313 (0.9209–1.627)	0.0392
Mx1		GTT TCC GAA GTG GAC ATC GCA	CCA TTC AGT AAT AGA GGG TGG GA	0.1703 (0.1163–0.3839)	1.140 (0.4724–2.399)	<0.0001
IFI6	Antiapoptotic (12, 63)	GGT CTG CGA TCC TGA ATG GG	TCA CTA TCG AGA TAC TTG TGG GT	0.8497 (0.4130–1.969)	5.150 (2.086–12.72)	0.0002
IFI27	Proapoptotic (56)	TGG CTC TGC CGT AGT TTT G	TCC TCC AAT CAC AAC TGT AGC A	0.3359 (0.1101–0.8334)	158.7 (10.34–533.5)	<0.0001
IFITM2	Proapoptotic (17)	ATG AAC CAC ATT GTG CAA ACC T	CCC AGC ATA GCC ACT TCC T	1.798 (1.167–2.780)	3.128 (2.105–4.960)	0.0015

[a] NS, not significant.

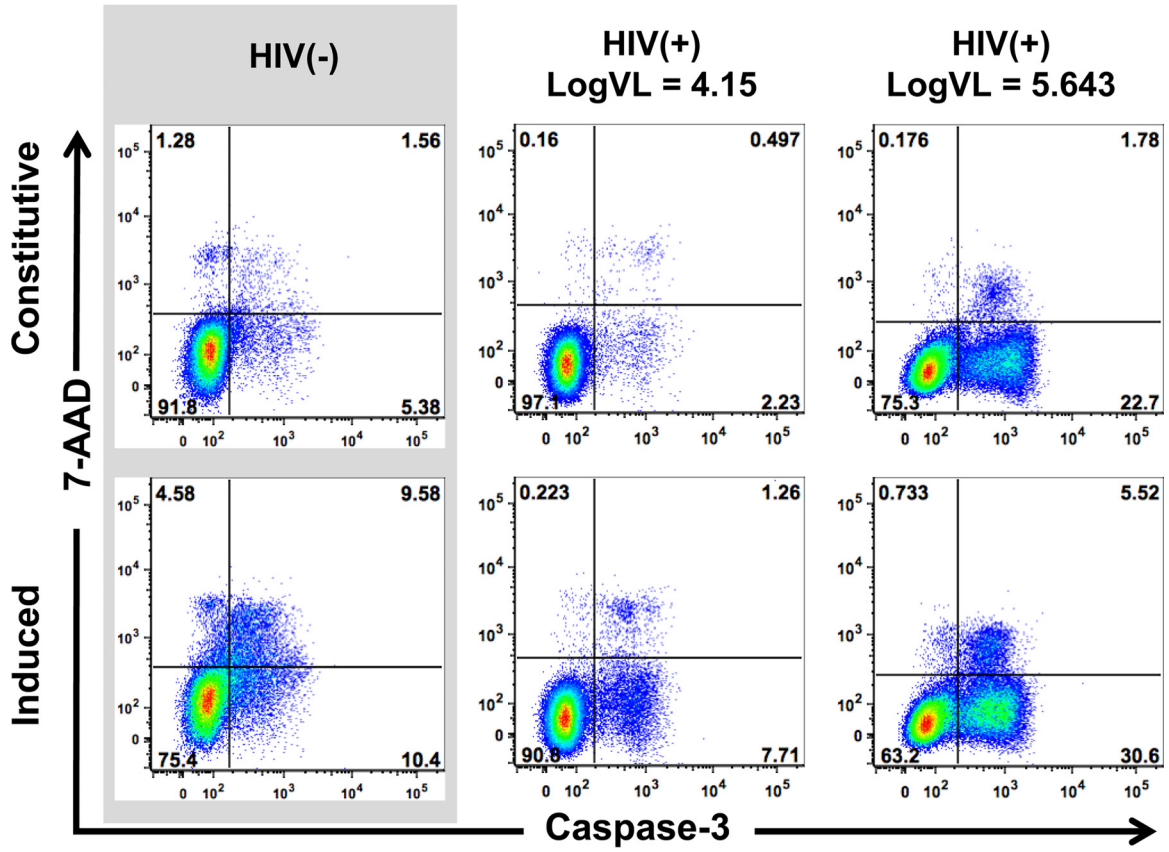

FIG 1 Monocyte apoptosis characterization. Representative 7-AAD/caspase-3 dot plots of purified monocytes from uninfected and HIV$^+$ (14,000 and 439,508 copies/ml) patients are shown. Plots represent overnight constitutive apoptosis (first row) and oxidative stress induced apoptosis (20 μM $CdCl_2$) (second row).

ear regressions (data not shown). Q-Q plot was used to examine normality. Residual plot was used to examine the equal variance assumption. The *t* value is the coefficient divided by its standard deviation. A larger *t* value associates with a smaller *P* value and more convincing evidence against the null hypothesis that the coefficient is zero. The F statistic stands for the F-test on the overall regression model. It tests for a significant linear regression relationship between the response variable and the predictor variables (Table 3).

RESULTS

Monocyte apoptosis is elevated in HIV-1 subjects with higher viremia. Monocyte constitutive and induced apoptosis was examined in a cohort of viremic patients (Table 1) with a wide range of viral loads (2,243 to 1,355,998 copies/ml) and CD4 counts (26 to 801 cells/mm^3) (Fig. 1 and 2). As expected, CD4 count was negatively associated with viral load ($P = 0.0012$; $R = -0.5255$).

Both constitutive and oxidative stress-induced apoptosis (20 μM $CdCl_2$) (42–45) showed a higher frequency of caspase-3-positive cells at viral loads above 40,000 ($\log_{10}$ 4.60) copies/ml (constitutive $P = 0.0034$; induced $P = 0.0002$) than values for subjects with lower-level viremia (Fig. 2A). Irrespective of viral load, increased T-cell apoptosis was observed in all HIV$^+$ patients compared to that for uninfected donors (data not shown). For all HIV$^+$ patients, constitutive and induced apoptosis were positively associated with viral load ($P = 0.0256$ and $R = 0.3883$ and $P = 0.0002$ $R = 0.5974$, respectively) and inversely associated with CD4 count ($P = 0.0128$ and $R = -0.4288$ and $P = 0.0464$ and $R = -0.3491$, respectively) (Fig. 2B and C). Supporting a threshold effect of viral load, the correlation of viral load with apoptosis was not present if restricted to only patients with loads lower or higher than 40,000 copies/ml (all *P* values > 0.05). Our data show that higher viral load is associated with increased constitutive and induced apoptosis in circulating monocytes.

Markers of innate immune activation are increased with HIV$^+$ infection but do not associate with change in monocyte apoptosis. Previous findings have described CD14^{++} CD16$^+$ intermediate monocytes (10–12, 46) and the plasma factors sCD14 (13, 14, 17, 47) and sCD163 (15, 16, 40, 48) as biomarkers of monocyte/macrophage activation and pathogenesis in SIV and HIV-1 disease. Therefore, we investigated the relationship between these variables and change in monocyte apoptosis with increasing viral load. We found that the CD14^{++} CD16$^+$ intermediate subset and plasma sCD163 concentrations were elevated in the HIV$^+$ group compared to controls (Fig. 3A, graphs 1 and 3), but we did not detect differences within the HIV$^+$ groups (Fig. 3B) or an association between these variables with viral load (Fig. 3C), monocyte apoptosis (Fig. 3D), or CD4 count (see Fig. S2 in the supplemental material). Conversely, plasma sCD14 concentration was associated with viral load (Fig. 3C) and CD4 count (see Fig. S2A in the supplemental material) but not monocyte apoptosis ($P = 0.1070$ [Fig. 3D]). Below a CD4 count of 500 cells/mm^3 (see Fig. S2B in the supplemental material), CD4 count demonstrated a strong negative correlation with sCD14 ($P < 0.0001$) and

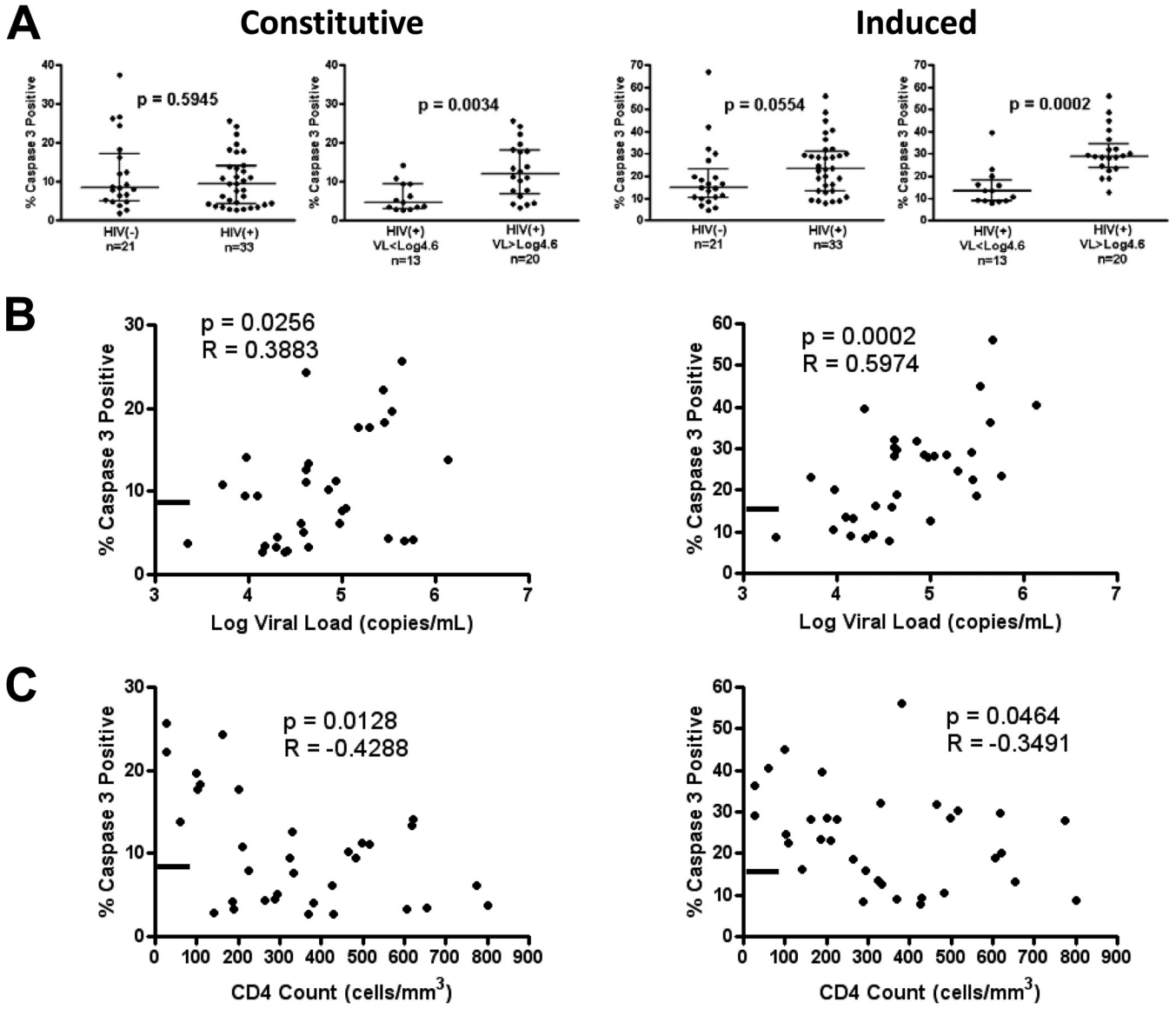

FIG 2 Monocyte apoptosis is elevated in patients above 40,000 copies/ml and associated with viral load and CD4 T cell count. (A) Groupwise comparison of constitutive (left) and induced (right) apoptosis in HIV^- versus HIV^+ individuals and HIV^+ patients below versus above 40,000 (log_{10} 4.6) copies/ml. (B and C) Spearman ranked correlation of viral load (B) and CD4 count (C) versus monocyte apoptosis levels in HIV^+ patients. The line on the *y* axis represents the median constitutive (8.48%) and induced (14.82%) apoptosis levels of the HIV^- group. Groupwise comparison displays median and interquartile range using the Mann-Whitney test (two tailed), with a *P* value of <0.05 considered significant. Spearman (two tailed) rho and *P* values are displayed.

trended with sCD163 ($P = 0.0657$). Taken together, data support the presence of monocyte activation with persistent sCD163 and $CD14^{++}$ $CD16^+$ monocytes (and an association of sCD14 with viremia and CD4) that is independent of changes in monocyte apoptosis with viral load.

Apoptosis-related ISG family gene expression is altered in association with viral load. Based on prior reports identifying key genes associated with monocyte apoptosis, such as Rb1 (18, 33), and type I interferon gene expression in monocytes from highly viremic HIV-1 patients (7, 8, 19), we focused on testing if functional changes in monocyte apoptosis were associated with changes in p53 (33, 49, 50), Bcl2/cytochrome *c* (51–55), and ISG (56–63) family expression due to their known apoptosis regulation functions (Table 2). Quantitative reverse transcription-PCR (RT-qPCR) analysis at time of isolation showed significantly higher Rb1 expression in the total HIV^+ group than in the HIV^- group ($P = 0.0100$) but no association with viral load, consistent with reports of Rb1 contributions to apoptosis resistance (33) in circulating monocytes during HIV infection. Within the Bcl2/cytochrome *c* genes analyzed, the HIV^+ group (relative to the HIV^- group) was characterized by lower Bcl-w ($P = 0.0169$) and higher cytochrome *c* gene expression ($P = 0.0392$), both with no association of gene expression with viral load. In contrast, Mx1 and the apoptosis-associated ISG12 members (IFI6, IFI27, and IFITM2) showed higher expression in the HIV^+ group relative to the HIV^- group, and IFI27 and IFITM2 showed higher expression in the HIV^+ group above 40,000 copies/ml relative to the HIV^+ group below 40,000 copies/ml (Fig. 4A). The apoptosis-related ISGs

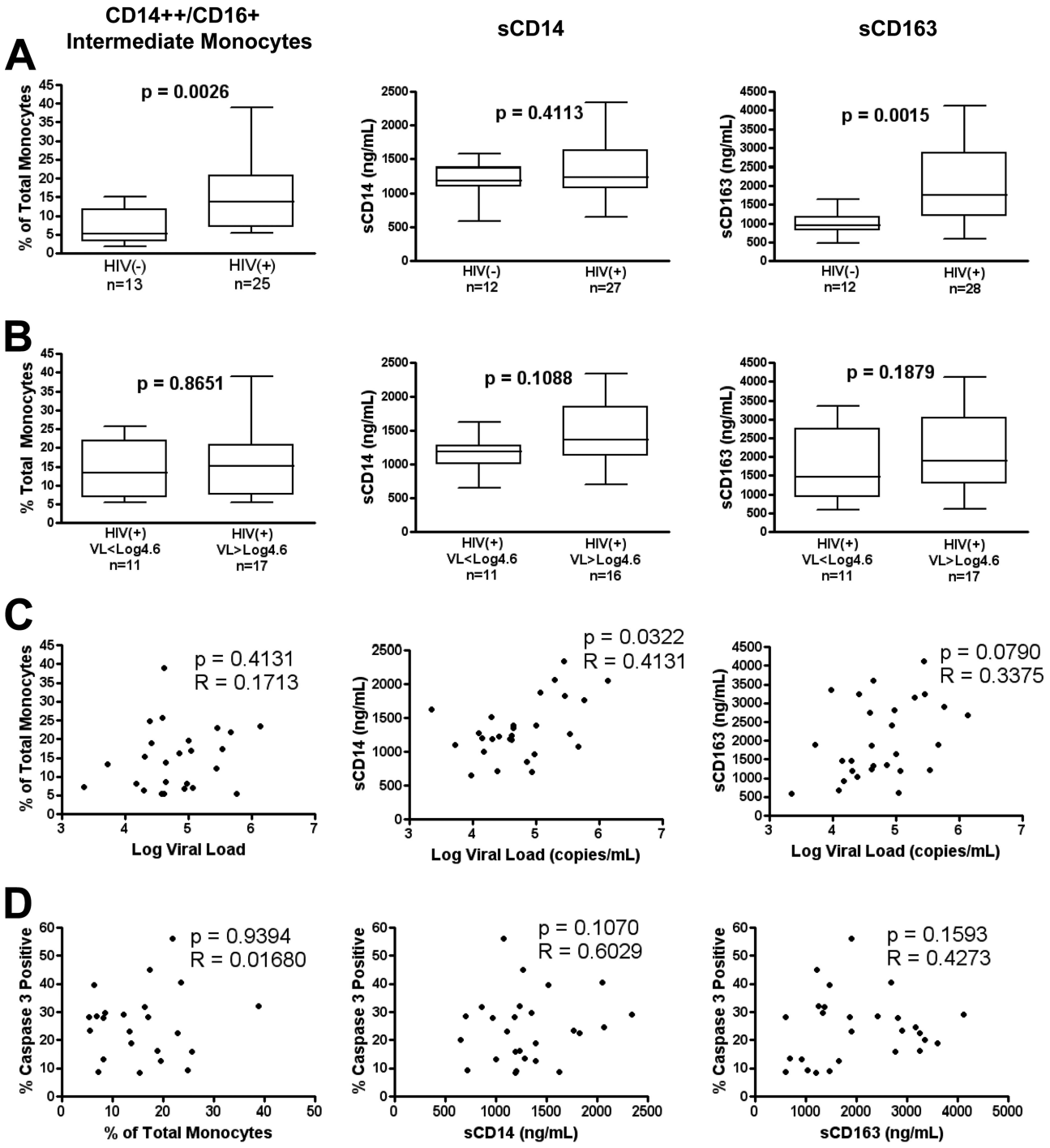

FIG 3 Monocyte/macrophage activation in HIV$^+$ patient cohort. (A and B) Groupwise comparison of percentage of intermediate CD14^{++} CD16$^+$ monocytes (left), plasma sCD14 (middle), and plasma sCD163 (right) in HIV$^-$ versus HIV$^+$ individuals (A) and HIV$^+$ patients below versus above 40,000 ($\log_{10}$ 4.6) copies/ml (B). (C and D) Spearman ranked correlation of viral load (C) and induced apoptosis (D) versus monocyte/macrophage activation metrics. Groupwise comparison displays median, interquartile range (box), and range (whiskers) using the Mann-Whitney test (two-tailed), with a *P* value of <0.05 considered significant. Spearman (two tailed) rho and *P* values are displayed.

(IFI6, IFI27, and IFITM2) were also positively associated with viral load (Fig. 4B), consistent with published data (7, 8, 19). Taken together, our data demonstrate a shift in monocyte gene expression with HIV-1 infection and increasing viral load consistent with apoptosis modulation.

Multivariate analysis identifies genes contributing to changes in constitutive and induced apoptosis in HIV infection. Although expression of genes within target families was correlated (p53, pro-apoptotic Bcl2 genes, and ISGs) (Fig. 5), only IFITM2 was associated with constitutive apoptosis, indicating that single-gene expression

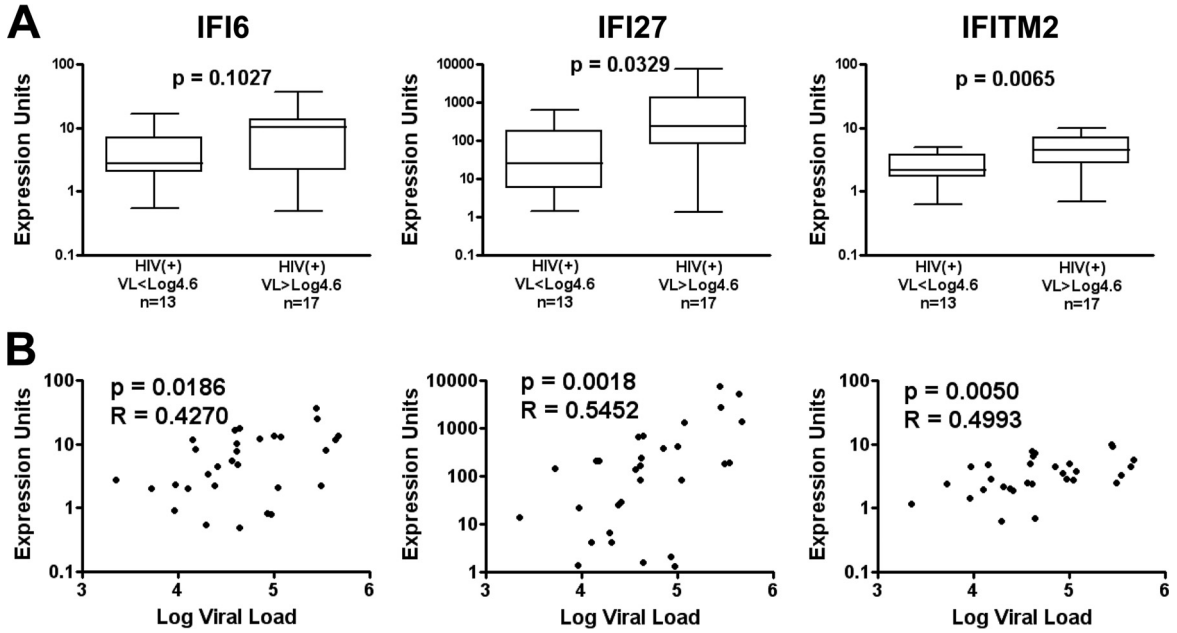

FIG 4 Monocyte ISG12 family expression is elevated in patients above 40,000 copies/ml and associated with viral load. (A) Groupwise comparison of IFI6, IFI27, and IFITM2 gene expression in HIV$^+$ patients below versus above 40,000 ($\log_{10}$ 4.6) copies/ml. (B) Spearman ranked correlation of viral load versus monocyte gene expression. Groupwise comparison displays median, interquartile range (box), and range (whiskers) using the Mann-Whitney test (two tailed), with a *P* value of <0.05 considered significant. Spearman (two tailed) rho and *P* values are displayed.

analysis could not a reflect change in both constitutive and induced apoptosis function. Multivariable stepwise regression modeling was applied to evaluate if the combination of viral load, CD4 count, and gene expression variables could generate a model for the distribution of constitutive and induced apoptosis responses observed in HIV-infected subjects. The adjusted R^2 rank method identified IFI27, IFITM2, Rb1, and Bcl2 expression as the best model to describe variance in constitutive apoptosis ($P = 3.77 \times 10^{-5}$; adjusted $R^2 = 0.5983$) (Table 3 and Fig. 6A). A reduction of this model showed that the key variables were IFI27 and Bcl2, accounting for 96.4% of the adjusted R^2 value. For oxidative stress-induced apoptosis, the model system identified log viral load, IFITM2, Rb1, and Bax expression ($P = 5.59 \times 10^{-5}$; adjusted $R^2 = 0.5996$) (Table 3 and Fig. 6B) with log viral load and Rb1 gene expression, representing 83.1% of the adjusted R^2 value. Taken together, the results showed that the shift in functional monocyte apoptosis observed with increasing viral load was associated with a multigene contribution, including changes in Rb1, ISG, and Bcl2 expression.

	LogVL	CD4	Rb1	MDM2	Bcl2	Bcl-w	Mcl-1	Bax	Bak1	Bik	CycS	Mx1	IFI6	IFI27	IFITM2	None	$CdCl_2$
LogVL	x	**-0.4121**	0.0826	0.2472	0.1591	0.2401	0.1756	**0.3709**	0.2036	-0.022	0.3587	**0.3716**	**0.453**	**0.551**	**0.5527**	**0.3941**	**0.6202**
CD4		x	**0.3758**	0.0781	0.034	-0.2138	0.1279	-0.1199	-0.0309	-0.0616	0.0287	-0.2992	-0.3473	**-0.4398**	-0.228	-0.3664	-0.3388
Rb1			x	**0.6013**	0.3224	0.1822	**0.4185**	**0.5257**	0.3175	0.3522	**0.6427**	**0.3958**	0.3499	0.1835	**0.5181**	0.0647	0.0781
MDM2				x	0.1893	**0.4354**	**0.6903**	**0.7161**	**0.535**	**0.3935**	**0.8154**	**0.6369**	**0.5177**	**0.5159**	**0.6792**	0.1608	0.1675
Bcl2					x	-0.0149	0.2534	0.2814	**0.4278**	0.2222	0.2685	0.2423	0.0096	-0.0509	0.3246	0.2828	0.1515
Bcl-w						x	**0.418**	0.3544	0.3335	0.495	0.232	**0.4011**	**0.5929**	**0.539**	**0.4616**	0.2071	-0.0109
Mcl-1							x	**0.5386**	**0.584**	0.2979	**0.62**	0.3028	0.1617	0.087	**0.4567**	0.2147	0.0576
Bax								x	**0.7055**	**0.4202**	**0.8469**	**0.5626**	**0.5564**	**0.4492**	**0.6814**	0.1542	0.0518
Bak1									x	**0.5813**	**0.6249**	**0.4354**	0.2819	0.1199	**0.4145**	0.1382	0.0354
Bik										x	**0.3842**	**0.5226**	**0.4594**	0.2369	0.3588	-0.0149	-0.1702
CycS											x	**0.4888**	**0.3829**	0.3201	**0.6076**	0.1706	0.2062
Mx1												x	**0.8394**	**0.7882**	**0.8394**	0.2485	0.2067
IFI6													x	**0.9088**	**0.7802**	0.1471	0.1435
IFI27														x	**0.7628**	0.1929	0.3108
IFITM2															x	**0.3717**	0.2939
None																x	**0.5319**
$CdCl_2$																	x

FIG 5 Gene expression correlation of p53, Bcl2, and ISG family genes in monocytes of HIV$^+$ donors. Shown is a Spearman ranked correlation matrix of clinical parameters (brown), p53 (pink), Bcl2 (blue), and ISG (green) family genes, as well as constitutive and induced apoptosis (purple). The results for the Spearman test (two tailed, unadjusted), with a *P* value of <0.05 considered significant (bold red type), and Spearman rho are displayed ($n = 30$).

TABLE 3 Multivariate analysis of HIV-1 monocyte apoptosis[a]

Apoptosis type	Statistic	Coefficient	Estimate	SE	95% CI	*t* value	*P* value
Constitutive		Intercept	6.445281	2.2119471	1.8695 to 11.0210	2.914	7.82E−03
		IFI27	0.003723	0.0008659	0.001932 to 0.005514	4.299	2.67E−04
		IFITM2	−1.24797	0.6839378	−2.6628 to 0.16686	−1.825	0.081066
		Rb1	0.393577	0.3363558	−0.3022 to 1.0894	1.17	2.54E−01
		Bcl2	1.811856	0.4172257	0.9488 to 2.6750	4.343	2.40E−04
Multiple R^2	0.6578						
Adjusted R^2	0.5983						
F statistic	11.05 on 4 and 23 DF						
P value	3.77E-05						
Induced		Intercept	−98.354	21.986	−143.9495 to −52.7577	−4.473	1.90E−04
		Log viral load	19.890	3.532	12.5647 to 27.2153	5.631	1.16E−05
		IFITM2	−5.899	4.277	−14.7694 to 2.9718	−1.379	0.18173
		Rb1	15.037	5.332	3.978022 to 26.0957065	2.820	0.00997
		Bax	−16.529	8.200	−33.534222 to 0.4762045	−2.016	0.0562
Multiple R^2	0.6612						
Adjusted R^2	0.5996						
F statistic	10.73 on 4 and 22 DF						
P value	5.59E-05						

[a] SE, standard error; CI, confidence interval; DF, degrees of freedom.

DISCUSSION

Here we show for the first time that monocyte apoptosis is elevated in patients with more than 40,000 copies/ml and negatively associated with CD4 count (Fig. 2). Our data suggest that a viral load below this threshold can modulate monocyte and macrophage activation, as indicated by change in sCD163 and $CD14^{++}$ $CD16^{+}$ monocytes, yet does not result in a rise in apoptosis until higher viral loads, clarifying conflicting reports of monocyte apoptosis in HIV infection (18, 30–33, 35, 41). Interestingly, our data suggest the presence of at least two distinct phases of monocyte/macrophage activation relative to viremia: (i) below 40,000 copies/ml, characterized by increases in plasma sCD163, the $CD14^{++}$ $CD16^{+}$ intermediate monocyte subset, Rb1 expression, and cell viability (as described in references 18, 32, and 33), and (ii) above 40,000 copies/ml, described here, characterized by increasing plasma sCD14 with viral load, high ISG expression, and elevated apoptosis.

Although monocyte type I interferon-stimulated gene expression (7, 8, 19) and monocyte activation markers (10–17, 40, 46–48) have been described as modulated during HIV-1 and SIV infection, the present study extends these data by showing that an elevation in apoptosis at higher viremia can be detected in spite of

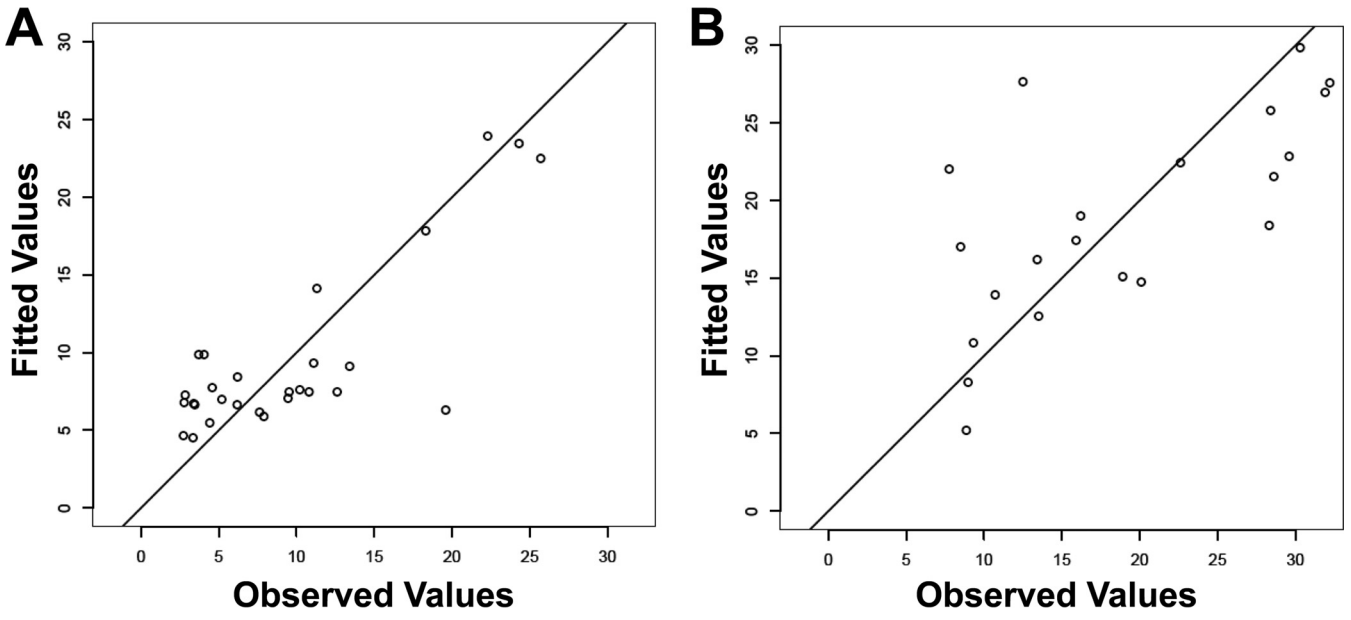

FIG 6 Multivariate analysis of monocyte apoptosis in HIV-1 viremic patients. Shown are the top models generated showing fitted versus observed constitutive (A) and induced (B) apoptosis by multivariate stepwise regression of clinical parameters and apoptosis gene expression.

active mechanisms of apoptosis resistance (i.e., higher zinc content and Rb1 expression) (18, 31, 32). Change in ISG expression and increasing sCD14 with viremia may evidence increasing microbial translocation, as microbial products were associated with interferon alpha activation in HIV-1 viremic patients (17) and may contribute to the shift in monocyte ISG expression and apoptosis induction (64, 65).

Previous studies have demonstrated elevated sCD14 in multiple comparisons of HIV^+ to HIV^- donors (14, 16, 17, 66–68), and while we demonstrated an association with viral load and CD4 count (Fig. 3C; see also Fig. S2 in the supplemental material), we did not detect a significant increase from the HIV^- to the HIV^+ group (Fig. 3A), which may reflect differences in sample size and the characteristics of the HIV^+ cohort. Interestingly, others have observed biphasic CD163 expression on $CD14^{++}$ $CD16^+$ monocytes relative to CD4 count (negative correlation below and positive correlation above 500 cells/mm^3) (69). Although we did not measure membrane CD163 expression, we observed a negative trend of CD4 count with sCD163, as well as a strong negative correlation with sCD14, in patients below 500 cells/μl (see Fig. S2 in the supplemental material), supporting these observations. We interpret this to mean that the reversal of monocyte activation upon ART-mediated suppression may vary qualitatively and temporally, as indicated by resolution of Rb1 protein expression (33), decreased $CD14^{++}$ $CD16^+$ monocyte levels when treated in early infection but not if treated in chronic infection (15), persistence of plasma sCD14 (16, 66, 68), and partial (incomplete) plasma sCD163 resolution (16, 70). Future longitudinal studies will be needed to establish the temporal relationship between monocyte activation variables described here in the context of disease progression and ART-mediated viral suppression.

In addition to the main study conclusion regarding impact of viral load, multivariable analysis highlighted candidate ISG and Bcl2 genes as potential contributors to the functional apoptosis shift when added to rising viral load and sustained Rb1 expression (Table 3 and Fig. 6). Members of the ISG12 family (56, 62) examined in this study, including IFI6 (57, 58), IFI27 (59), and IFITM2 (60), have described apoptosis regulation functions. Of interest, IFITM2 was the only gene associated with apoptosis outcome at the single-gene level (Fig. 5) and IFITM2 and Rb1 were present in both models (Table 3 and Fig. 6), supporting specific candidate roles of these genes as determinants of monocyte apoptosis in HIV-infected subjects. The impact of HIV-1 on Bcl2-mediated apoptosis in the CD4 compartment is also well described (reviewed in reference 39), and the effect on non-CD4 cell types, namely, CD8 T cells (71), dendritic cells (72), and now monocytes, suggests a global impact of HIV-1 viremia and immune activation on Bcl2-mediated apoptosis regulation. In addition, it has been established that Rb1 can override p53-mediated apoptosis induction *in vitro* (50), yet it remains to be determined whether Bax and ISG12 family expression can override antiapoptotic Rb1 expression as suggested by our data. The multiple genes measured *ex vivo* as contributing to apoptosis regulation makes it highly unlikely that the functional phenotype can be accounted for by any one gene. However, future work could determine how the described proapoptotic (IFI27, IFITM2, and Bax) and antiapoptotic (Rb1 and Bcl2) proteins exert regulation of apoptosis when coexpressed to define overall dominance or an additive effect.

Our data do not address the potential impact of age and gender on monocyte apoptosis (14, 73, 74). Both HIV^- and HIV^+ groups represent similar gender (no more than 25% female) and age distributions, but our cohort is limited in the representation of females and aged individuals (see Table S1 in the supplemental material). Future studies will need to address the impact of age and gender on monocyte apoptosis and apoptosis gene expression. Despite lower median apoptosis levels in the HIV^+ group with $<$40,000 copies/ml than in the HIV^- group, no significant difference was detected, in contrast to previous studies (18, 32, 33). We interpret this difference to reflect the methods used, as the current study's apoptosis assay was based on overnight incubations, compared to 6 h postisolation, as done previously.

Although we interpret a direct role for target genes in apoptosis, a limitation of this study is the lack of single- to multiple-gene knockdowns in monocytes to establish the conclusive role of target genes. However, the well-established functional role of proapoptotic genes identified in this work as contributing to apoptosis lends support to the notion that their increased expression may impact apoptosis. Also, while we focused on the relationship between apoptosis and apoptosis-related gene families expressed within cells (p53, ISG, and Bcl2), our data do not exclude contributions by added external mechanisms *in vivo* affecting total monocyte numbers, such as *de novo* production and turnover described to occur in SIV infection (40, 41) or external factors such as soluble TRAIL in viremic serum (35, 38) or increased TRAIL-mediated apoptosis (30, 34, 37, 75).

Our data join an increasing body of evidence suggesting that high viral load and low CD4 count may be associated with changes in monocyte functional responses, including greater monocyte turnover (associated with plasma sCD163) (40, 41), tissue migration (40, 41, 76), and macrophage apoptosis in tissue (41). This study complements studies with SIV-infected macaques (using *in vivo* bromodeoxyuridine [BrdU] labeling) in which disease progression (i.e., high viral load) was associated with increased monocyte turnover, which may be associated with higher levels of apoptosis (40, 41). Indeed, an increase in monocyte apoptosis with higher viremia may be associated with the onset of pathology, as suggested by observations of high constitutive monocyte apoptosis and proapoptotic Bcl2 family expression in SIV-infected macaques during pathogenic SIV macaque infection but not in nonpathogenic African green monkey infection (30).

In summary, we establish a shift in monocyte functional apoptosis and gene expression in association with high HIV-1 viral load and low CD4 count, which may bear on mechanisms for immunodeficiency, HIV replication, and/or HIV reservoir retention in HIV-1 disease.

ACKNOWLEDGMENTS

This study was supported by U.S. National Institutes of Health grant R01 AI073219, the Philadelphia Foundation (Robert I. Jacobs Fund), Henry S. Miller, Jr., J. Kenneth Nimblett, the Commonwealth Universal Research Enhancement Program, the Pennsylvania Department of Health, the Penn Center for AIDS Research (P30AI045008), and the NIH-T32 HIV Pathogenesis Training Grant through the University of Pennsylvania. Support for shared resources utilized in this study was provided by Cancer Center Support Grant (CCSG) P30CA010815 to The Wistar Institute.

The content of this article is solely the responsibility of the authors and does not necessarily represent the official views of the National Institutes of Health.

We thank the Wistar Genomics Facility and Jeffery Faust (Wistar Flow Cytometry) for help with experiments and Wistar phlebotomist Deborah Davis for blood donor recruitment.

REFERENCES

1. **Alkhatib G.** 2009. The biology of CCR5 and CXCR4. Curr Opin HIV AIDS **4:**96–103. http://dx.doi.org/10.1097/COH.0b013e328324bbec.
2. **Guadalupe M, Reay E, Sankaran S, Prindiville T, Flamm J, McNeil A, Dandekar S.** 2003. Severe CD4+ T-cell depletion in gut lymphoid tissue during primary human immunodeficiency virus type 1 infection and substantial delay in restoration following highly active antiretroviral therapy. J Virol **77:**11708–11717. http://dx.doi.org/10.1128/JVI.77.21.11708-11717.2003.
3. **Badley AD, Pilon AA, Landay A, Lynch DH.** 2000. Mechanisms of HIV-associated lymphocyte apoptosis. Blood **96:**2951–2964.
4. **Yue FY, Kovacs CM, Dimayuga RC, Gu XX, Parks P, Kaul R, Ostrowski MA.** 2005. Preferential apoptosis of HIV-1-specific CD4+ T cells. J Immunol **174:**2196–2204. http://dx.doi.org/10.4049/jimmunol.174.4.2196.
5. **Gekonge B, Giri MS, Kossenkov AV, Nebozyhn M, Yousef M, Mounzer K, Showe L, Montaner LJ.** 2012. Constitutive gene expression in monocytes from chronic HIV-1 infection overlaps with acute Toll-like receptor induced monocyte activation profiles. PLoS One **7:**e41153. http://dx.doi.org/10.1371/journal.pone.0041153.
6. **Rempel H, Sun B, Calosing C, Abadjian L, Monto A, Pulliam L.** 2013. Monocyte activation in HIV/HCV coinfection correlates with cognitive impairment. PLoS One **8:**e55776. http://dx.doi.org/10.1371/journal.pone.0055776.
7. **Pulliam L, Rempel H, Sun B, Abadjian L, Calosing C, Meyerhoff DJ.** 2011. A peripheral monocyte interferon phenotype in HIV infection correlates with a decrease in MRS metabolite concentrations. AIDS **25:**1721–1726. http://dx.doi.org/10.1097/QAD.0b013e328349f022.
8. **Rempel H, Sun B, Calosing C, Pillai SK, Pulliam L.** 2010. Interferon-α drives monocyte gene expression in chronic unsuppressed HIV-1 infection. AIDS **24:**1415–1423. http://dx.doi.org/10.1097/QAD.0b013e32833ac623.
9. **Pulliam L, Sun B, Rempel H.** 2004. Invasive chronic inflammatory monocyte phenotype in subjects with high HIV-1 viral load. J Neuroimmunol **157:**93–98. http://dx.doi.org/10.1016/j.jneuroim.2004.08.039.
10. **Pulliam L, Gascon R, Stubblebine M, McGuire D, McGrath M.** 1997. Unique monocyte subset in patients with AIDS dementia. Lancet **349:**692–695. http://dx.doi.org/10.1016/S0140-6736(96)10178-1.
11. **Ellery PJ, Tippett E, Chiu YL, Paukovics G, Cameron PU, Solomon A, Lewin SR, Gorry PR, Jaworowski A, Greene WC, Sonza S, Crowe SM.** 2007. The CD16+ monocyte subset is more permissive to infection and preferentially harbors HIV-1 in vivo. J Immunol **178:**6581–6589. http://dx.doi.org/10.4049/jimmunol.178.10.6581.
12. **Williams K, Burdo TH.** 2012. Monocyte mobilization, activation markers, and unique macrophage populations in the brain: observations from SIV infected monkeys are informative with regard to pathogenic mechanisms of HIV infection in humans. J Neuroimmune Pharmacol **7:**363–371. http://dx.doi.org/10.1007/s11481-011-9330-3.
13. **Sandler NG, Wand H, Roque A, Law M, Nason MC, Nixon DE, Pedersen C, Ruxrungtham K, Lewin SR, Emery S, Neaton JD, Brenchley JM, Deeks SG, Sereti I, Douek DC.** 2011. Plasma levels of soluble CD14 independently predict mortality in HIV infection. J Infect Dis **203:**780–790. http://dx.doi.org/10.1093/infdis/jiq118.
14. **Martin GE, Gouillou M, Hearps AC, Angelovich TA, Cheng AC, Lynch F, Cheng WJ, Paukovics G, Palmer CS, Novak RM, Jaworowski A, Landay AL, Crowe SM.** 2013. Age-associated changes in monocyte and innate immune activation markers occur more rapidly in HIV infected women. PLoS One **8:**e55279. http://dx.doi.org/10.1371/journal.pone.0055279.
15. **Burdo TH, Lo J, Abbara S, Wei J, DeLelys ME, Preffer F, Rosenberg ES, Williams KC, Grinspoon S.** 2011. Soluble CD163, a novel marker of activated macrophages, is elevated and associated with noncalcified coronary plaque in HIV-infected patients. J Infect Dis **204:**1227–1236. http://dx.doi.org/10.1093/infdis/jir520.
16. **Burdo TH, Lentz MR, Autissier P, Krishnan A, Halpern E, Letendre S, Rosenberg ES, Ellis RJ, Williams KC.** 2011. Soluble CD163 made by monocyte/macrophages is a novel marker of HIV activity in early and chronic infection prior to and after anti-retroviral therapy. J Infect Dis **204:**154–163. http://dx.doi.org/10.1093/infdis/jir214.
17. **Brenchley JM, Price DA, Schacker TW, Asher TE, Silvestri G, Rao S, Kazzaz Z, Bornstein E, Lambotte O, Altmann D, Blazar BR, Rodriguez B, Teixeira-Johnson L, Landay A, Martin JN, Hecht FM, Picker LJ, Lederman MM, Deeks SG, Douek DC.** 2006. Microbial translocation is a cause of systemic immune activation in chronic HIV infection. Nat Med **12:**1365–1371. http://dx.doi.org/10.1038/nm1511.
18. **Giri MS, Nebozyhn M, Raymond A, Gekonge B, Hancock A, Creer S, Nicols C, Yousef M, Foulkes AS, Mounzer K, Shull J, Silvestri G, Kostman J, Collman RG, Showe L, Montaner LJ.** 2009. Circulating monocytes in HIV-1-infected viremic subjects exhibit an antiapoptosis gene signature and virus- and host-mediated apoptosis resistance. J Immunol **182:**4459–4470. http://dx.doi.org/10.4049/jimmunol.0801450.
19. **Tilton JC, Johnson AJ, Luskin MR, Manion MM, Yang J, Adelsberger JW, Lempicki RA, Hallahan CW, McLaughlin M, Mican JM, Metcalf JA, Iyasere C, Connors M.** 2006. Diminished production of monocyte proinflammatory cytokines during human immunodeficiency virus viremia is mediated by type I interferons. J Virol **80:**11486–11497. http://dx.doi.org/10.1128/JVI.00324-06.
20. **Boasso A, Hardy AW, Landay AL, Martinson JL, Anderson SA, Dolan MJ, Clerici M, Shearer GM.** 2008. PDL-1 upregulation on monocytes and T cells by HIV via type I interferon: restricted expression of type I interferon receptor by CCR5-expressing leukocytes. Clin Immunol **129:**132–144. http://dx.doi.org/10.1016/j.clim.2008.05.009.
21. **Amirayan-Chevillard N, Tissot-Dupont H, Capo C, Brunet C, Dignat-George F, Obadia Y, Gallais H, Mege JL.** 2000. Impact of highly active anti-retroviral therapy (HAART) on cytokine production and monocyte subsets in HIV-infected patients. Clin Exp Immunol **120:**107–112. http://dx.doi.org/10.1046/j.1365-2249.2000.01201.x.
22. **Cozzi-Lepri A, French MA, Baxter J, Okhuysen P, Plana M, Neuhaus J, Landay A.** 2011. Resumption of HIV replication is associated with monocyte/macrophage derived cytokine and chemokine changes: results from a large international clinical trial. AIDS **25:**1207–1217. http://dx.doi.org/10.1097/QAD.0b013e3283471f10.
23. **Zhu T, Muthui D, Holte S, Nickle D, Feng F, Brodie S, Hwangbo Y, Mullins JI, Corey L.** 2002. Evidence for human immunodeficiency virus type 1 replication in vivo in CD14+ monocytes and its potential role as a source of virus in patients on highly active antiretroviral therapy. J Virol **76:**707–716. http://dx.doi.org/10.1128/JVI.76.2.707-716.2002.
24. **Lewin SR, Kirihara J, Sonza S, Irving L, Mills J, Crowe SM.** 1998. HIV-1 DNA and mRNA concentrations are similar in peripheral blood monocytes and alveolar macrophages in HIV-1-infected individuals. AIDS **12:**719–727. http://dx.doi.org/10.1097/00002030-199807000-00008.
25. **Giri MS, Nebozhyn M, Showe L, Montaner LJ.** 2006. Microarray data on gene modulation by HIV-1 in immune cells: 2000–2006. J Leukoc Biol **80:**1031–1043. http://dx.doi.org/10.1189/jlb.0306157.
26. **Rempel H, Calosing C, Sun B, Pulliam L.** 2008. Sialoadhesin expressed on IFN-induced monocytes binds HIV-1 and enhances infectivity. PLoS One **3:**e1967. http://dx.doi.org/10.1371/journal.pone.0001967.
27. **Said EA, Dupuy FP, Trautmann L, Zhang Y, Shi Y, El-Far M, Hill BJ, Noto A, Ancuta P, Peretz Y, Fonseca SG, Van Grevenynghe J, Boulassel MR, Bruneau J, Shoukry NH, Routy J-P, Douek DC, Haddad EK, Sekaly R-P.** 2010. Programmed death-1-induced interleukin-10 production by monocytes impairs CD4+ T cell activation during HIV infection. Nat Med **16:**452–459. http://dx.doi.org/10.1038/nm.2106.
28. **Meier A, Bagchi A, Sidhu HK, Alter G, Suscovich TJ, Kavanagh DG, Streeck H, Brockman MA, LeGall S, Hellman J, Altfeld M.** 2008. Upregulation of PD-L1 on monocytes and dendritic cells by HIV-1 derived TLR ligands. AIDS **22:**655–658. http://dx.doi.org/10.1097/QAD.0b013e3282f4de23.
29. **Zheng L, Yang Y, Guocai L, Pauza CD, Salvato MS.** 2007. HIV Tat protein increases Bcl-2 expression in monocytes which inhibits monocyte apoptosis induced by tumor necrosis factor-alpha-related apoptosis-induced ligand. Intervirology **50:**224–228. http://dx.doi.org/10.1159/000100565.
30. **Laforge M, Campillo-Gimenez L, Monceaux V, Cumont MC, Hurtrel B, Corbeil J, Zaunders J, Elbim C, Estaquier J.** 2011. HIV/SIV infection primes monocytes and dendritic cells for apoptosis. PLoS Pathog **7:**e1002087. http://dx.doi.org/10.1371/journal.ppat.1002087.
31. **Swingler S, Mann AM, Zhou J, Swingler C, Stevenson M.** 2007. Apoptotic killing of HIV-1-infected macrophages is subverted by the viral envelope glycoprotein. PLoS Pathog **3:**e134. http://dx.doi.org/10.1371/journal.ppat.0030134.
32. **Raymond AD, Gekonge B, Giri MS, Hancock A, Papasavvas E, Chehimi J, Kossevkov AV, Nicols C, Yousef M, Mounzer K, Shull J, Kostman J, Showe L, Montaner LJ.** 2010. Increased metallothionein gene expression, zinc, and zinc-dependent resistance to apoptosis in circulating monocytes during HIV viremia. J Leukoc Biol **88:**589–596. http://dx.doi.org/10.1189/jlb.0110051.
33. **Gekonge B, Raymond AD, Yin X, Kostman J, Mounzer K, Collman RG,**

Showe L, Montaner LJ. 2012. Retinoblastoma protein induction by HIV viremia or CCR5 in monocytes exposed to HIV-1 mediates protection from activation-induced apoptosis: ex vivo and in vitro study. J Leukoc Biol **92:**397–405. http://dx.doi.org/10.1189/jlb.1111552.
34. **Zhu DM, Shi J, Liu S, Liu Y, Zheng D.** 2011. HIV infection enhances TRAIL-induced cell death in macrophage by down-regulating decoy receptor expression and generation of reactive oxygen species. PLoS One **6:**e18291. http://dx.doi.org/10.1371/journal.pone.0018291.
35. **Alhetheel A, Yakubtsov Y, Abdkader K, Sant N, Diaz-Mitoma F, Kumar A, Kryworuchko M.** 2008. Amplification of the signal transducer and activator of transcription I signaling pathway and its association with apoptosis in monocytes from HIV-infected patients. AIDS **22:**1137–1144. http://dx.doi.org/10.1097/QAD.0b013e3283013d42.
36. **Baruchel S, Wainberg MA.** 1992. The role of oxidative stress in disease progression in individuals infected by the human immunodeficiency virus. J Leukoc Biol **52:**111–114.
37. **Huang Y, Walstrom A, Zhang L, Zhao Y, Cui M, Ye L, Zheng JC.** 2009. Type I interferons and interferon regulatory factors regulate TNF-related apoptosis-inducing ligand (TRAIL) in HIV-1-infected macrophages. PLoS One **4:**e5397. http://dx.doi.org/10.1371/journal.pone.0005397.
38. **Herbeuval JP, Boasso A, Grivel JC, Hardy AW, Anderson SA, Dolan MJ, Chougnet C, Lifson JD, Shearer GM.** 2005. TNF-related apoptosis-inducing ligand (TRAIL) in HIV-1-infected patients and its in vitro production by antigen-presenting cells. Blood **105:**2458–2464. http://dx.doi.org/10.1182/blood-2004-08-3058.
39. **Cummins NW, Badley AD.** 2010. Mechanisms of HIV-associated lymphocyte apoptosis: 2010. Cell Death Dis **1:**e99. http://dx.doi.org/10.1038/cddis.2010.77.
40. **Burdo TH, Soulas C, Orzechowski K, Button J, Krishnan A, Sugimoto C, Alvarez X, Kuroda MJ, Williams KC.** 2010. Increased monocyte turnover from bone marrow correlates with severity of SIV encephalitis and CD163 levels in plasma. PLoS Pathog **6:**e1000842. http://dx.doi.org/10.1371/journal.ppat.1000842.
41. **Hasegawa A, Liu H, Ling B, Borda JT, Alvarez X, Sugimoto C, Vinet-Oliphant H, Kim WK, Williams KC, Ribeiro RM, Lackner AA, Veazey RS, Kuroda MJ.** 2009. The level of monocyte turnover predicts disease progression in the macaque model of AIDS. Blood **114:**2917–2925. http://dx.doi.org/10.1182/blood-2009-02-204263.
42. **Li M.** 2000. Apoptosis induced by cadmium in human lymphoma U937 cells through Ca2+-calpain and caspase-mitochondria-dependent pathways. J Biol Chem **275:**39702–39709. http://dx.doi.org/10.1074/jbc.M007369200.
43. **Galán A.** 2000. Stimulation of p38 mitogen-activated protein kinase is an early regulatory event for the cadmium-induced apoptosis in human promonocytic cells. J Biol Chem **275:**11418–11424. http://dx.doi.org/10.1074/jbc.275.15.11418.
44. **Miguel BG, Rodriguez ME, Aller P, Martinez AM, Mata F.** 2005. Regulation of cadmium-induced apoptosis by PKCδ in U937 human promonocytic cells. Biochim Biophys Acta **1743:**215–222. http://dx.doi.org/10.1016/j.bbamcr.2004.10.011.
45. **Sancho P, Fernández C, Yuste VJ, Amrán D, Ramos AM, de Blas E, Susin SA, Aller P.** 2006. Regulation of apoptosis/necrosis execution in cadmium-treated human promonocytic cells under different forms of oxidative stress. Apoptosis **11:**673–686. http://dx.doi.org/10.1007/s10495-006-5879-3.
46. **Kim WK, Sun Y, Do H, Autissier P, Halpern EF, Piatak M, Lifson JD, Burdo TH, McGrath MS, Williams K.** 2010. Monocyte heterogeneity underlying phenotypic changes in monocytes according to SIV disease stage. J Leukoc Biol **87:**557–567. http://dx.doi.org/10.1189/jlb.0209082.
47. **Romero-Sánchez M, Gonzalez-Serna A, Pacheco YM, Ferrando-Martinez S, Machmach K, Garcia-Garcia M, Alvarez-Rios AI, Vidal F, Leal M, Ruiz-Mateos E.** 2012. Different biological significance of sCD14 and LPS in HIV-infection: importance of the immunovirology stage and association with HIV-disease progression markers. J Infect **65:**431–438. http://dx.doi.org/10.1016/j.jinf.2012.06.008.
48. **Walker JA, Sulciner ML, Misgen KD, Miller AD, Burdo TH, Williams K.** February 2014. Elevated numbers of CD163+ macrophages in hearts of SIV infected monkeys correlates with cardiac pathology and fibrosis. AIDS Res Hum Retroviruses http://dx.doi.org/10.1089/AID.2013.0268.
49. **Haupt Y, Rowan S, Oren M.** 1995. p53-mediated apoptosis in HeLa cells can be overcome by excess pRB. Oncogene **10:**1563–1571.
50. **Shinohara H, Zhou J, Yoshikawa K, Yazumi S, Ko K, Yamaoka Y, Mizukami T, Yoshida T, Akinaga S, Tamaoki T, Motoda H, Benedict WF, Takahashi R.** 2000. Retinoblastoma protein-initiated cellular growth arrest overcomes the ability of cotransfected wild-type p53 to induce apoptosis. Br J Cancer **83:**1039–1046. http://dx.doi.org/10.1054/bjoc.2000.1411.
51. **Youle RJ, Strasser A.** 2008. The BCL-2 protein family: opposing activities that mediate cell death. Nat Rev Mol Cell Biol **9:**47–59. http://dx.doi.org/10.1038/nrm2308.
52. **Chipuk JE, Moldoveanu T, Llambi F, Parsons MJ, Green DR.** 2010. The BCL-2 family reunion. Mol Cell **37:**299–310. http://dx.doi.org/10.1016/j.molcel.2010.01.025.
53. **Ola MS, Nawaz M, Ahsan H.** 2011. Role of Bcl-2 family proteins and caspases in the regulation of apoptosis. Mol Cell Biochem **351:**41–58. http://dx.doi.org/10.1007/s11010-010-0709-x.
54. **Jiang X, Wang X.** 2004. Cytochrome C-mediated apoptosis. Annu Rev Biochem **73:**87–106. http://dx.doi.org/10.1146/annurev.biochem.73.011303.073706.
55. **Ow YP, Green DR, Hao Z, Mak TW.** 2008. Cytochrome c: functions beyond respiration. Nat Rev Mol Cell Biol **9:**532–542. http://dx.doi.org/10.1038/nrm2434.
56. **Martensen PM, Justesen J.** 2004. Small ISGs coming forward. J Interferon Cytokine Res **24:**1–19. http://dx.doi.org/10.1089/107999004772719864.
57. **Tahara E, Tahara H, Kanno M, Naka K, Takeda Y, Matsuzaki T, Yamazaki R, Ishihara H, Yasui W, Barrett JC, Ide T, Tahara E.** 2005. G1P3, an interferon inducible gene 6-16, is expressed in gastric cancers and inhibits mitochondrial-mediated apoptosis in gastric cancer cell line TMK-1 cell. Cancer Immunol Immunother **54:**729–740. http://dx.doi.org/10.1007/s00262-004-0645-2.
58. **Cheriyath V, Glaser KB, Waring JF, Baz R, Hussein MA, Borden EC.** 2007. G1P3, an IFN-induced survival factor, antagonizes TRAIL-induced apoptosis in human myeloma cells. J Clin Invest **117:**3107–3117. http://dx.doi.org/10.1172/JCI31122.
59. **Rosebeck S, Leaman DW.** 2008. Mitochondrial localization and pro-apoptotic effects of the interferon-inducible protein ISG12a. Apoptosis **13:**562–572. http://dx.doi.org/10.1007/s10495-008-0190-0.
60. **Daniel-Carmi V, Makovitzki-Avraham E, Reuven E-M, Goldstein I, Zilkha N, Rotter V, Tzehoval E, Eisenbach L.** 2009. The human1-8D gene (IFITM2) is a novel p53 independent pro-apoptotic gene. Int J Cancer **125:**2810–2819. http://dx.doi.org/10.1002/ijc.24669.
61. **Brass AL, Huang IC, Benita Y, John SP, Krishnan MN, Feeley EM, Ryan BJ, Weyer JL, van der Weyden L, Fikrig E, Adams DJ, Xavier RJ, Farzan M, Elledge SJ.** 2009. The IFITM proteins mediate cellular resistance to influenza A H1N1 virus, West Nile virus, and dengue virus. Cell **139:**1243–1254. http://dx.doi.org/10.1016/j.cell.2009.12.017.
62. **Cheriyath V, Leaman DW, Borden EC.** 2011. Emerging roles of FAM14 family members (G1P3/ISG 6-16 and ISG12/IFI27) in innate immunity and cancer. J Interferon Cytokine Res **31:**173–181. http://dx.doi.org/10.1089/jir.2010.0105.
63. **Lu J, Pan Q, Rong L, Liu SL, Liang C.** 2011. The IFITM proteins inhibit HIV-1 infection. J Virol **85:**2126–2137. http://dx.doi.org/10.1128/JVI.01531-10.
64. **Malcolm KC, Worthen GS.** 2003. Lipopolysaccharide stimulates p38-dependent induction of antiviral genes in neutrophils independently of paracrine factors. J Biol Chem **278:**15693–15701. http://dx.doi.org/10.1074/jbc.M212033200.
65. **Rustagi A, Gale M, Jr.** 2014. Innate antiviral immune signaling, viral evasion and modulation by HIV-1. J Mol Biol **426:**1161–1177. http://dx.doi.org/10.1016/j.jmb.2013.12.003.
66. **Lederman MM, Calabrese L, Funderburg NT, Clagett B, Medvik K, Bonilla H, Gripshover B, Salata RA, Taege A, Lisgaris M, McComsey GA, Kirchner E, Baum J, Shive C, Asaad R, Kalayjian RC, Sieg SF, Rodriguez B.** 2011. Immunologic failure despite suppressive antiretroviral therapy is related to activation and turnover of memory CD4 cells. J Infect Dis **204:**1217–1226. http://dx.doi.org/10.1093/infdis/jir507.
67. **Bukh AR, Melchjorsen J, Offersen R, Jensen JM, Toft L, Stovring H, Ostergaard L, Tolstrup M, Sogaard OS.** 2011. Endotoxemia is associated with altered innate and adaptive immune responses in untreated HIV-1 infected individuals. PLoS One **6:**e21275. http://dx.doi.org/10.1371/journal.pone.0021275.
68. **Lichtfuss GF, Meehan AC, Cheng WJ, Cameron PU, Lewin SR, Crowe SM, Jaworowski A.** 2011. HIV inhibits early signal transduction events triggered by CD16 cross-linking on NK cells, which are important for antibody-dependent cellular cytotoxicity. J Leukoc Biol **89:**149–158. http://dx.doi.org/10.1189/jlb.0610371.
69. **Tippett E, Cheng WJ, Westhorpe C, Cameron PU, Brew BJ, Lewin SR, Jaworowski A, Crowe SM.** 2011. Differential expression of CD163 on

monocyte subsets in healthy and HIV-1 infected individuals. PLoS One **6:**e19968. http://dx.doi.org/10.1371/journal.pone.0019968.

70. **Lichtfuss GF, Cheng WJ, Farsakoglu Y, Paukovics G, Rajasuriar R, Velayudham P, Kramski M, Hearps AC, Cameron PU, Lewin SR, Crowe SM, Jaworowski A.** 2012. Virologically suppressed HIV patients show activation of NK cells and persistent innate immune activation. J Immunol **189:**1491–1499. http://dx.doi.org/10.4049/jimmunol.1200458.
71. **Yan J, Sabbaj S, Bansal A, Amatya N, Shacka JJ, Goepfert PA, Heath SL.** 2013. HIV-specific CD8+ T cells from elite controllers are primed for survival. J Virol **87:**5170–5181. http://dx.doi.org/10.1128/JVI.02379-12.
72. **Dillon SM, Friedlander LJ, Rogers LM, Meditz AL, Folkvord JM, Connick E, McCarter MD, Wilson CC.** 2011. Blood myeloid dendritic cells from HIV-1-infected individuals display a proapoptotic profile characterized by decreased Bcl-2 levels and by caspase-3+ frequencies that are associated with levels of plasma viremia and T cell activation in an exploratory study. J Virol **85:**397–409. http://dx.doi.org/10.1128/JVI.01118-10.
73. **Hearps AC, Angelovich TA, Jaworowski A, Mills J, Landay AL, Crowe SM.** 2011. HIV infection and aging of the innate immune system. Sex Health **8:**453–464. http://dx.doi.org/10.1071/SH11028.
74. **Hearps AC, Martin GE, Angelovich TA, Cheng WJ, Maisa A, Landay AL, Jaworowski A, Crowe SM.** 2012. Aging is associated with chronic innate immune activation and dysregulation of monocyte phenotype and function. Aging Cell **11:**867–875. http://dx.doi.org/10.1111/j.1474-9726.2012.00851.x.
75. **Huang Y, Erdmann N, Peng H, Herek S, Davis JS, Luo X, Ikezu T, Zheng J.** 2006. TRAIL-mediated apoptosis in HIV-1-infected macrophages is dependent on the inhibition of Akt-1 phosphorylation. J Immunol **177:**2304–2313. http://dx.doi.org/10.4049/jimmunol.177.4.2304.
76. **Allers K, Fehr M, Conrad K, Epple HJ, Schurmann D, Geelhaar-Karsch A, Schinnerling K, Moos V, Schneider T.** 2014. Macrophages accumulate in the gut mucosa of untreated HIV-infected patients. J Infect Dis **209:**739–748. http://dx.doi.org/10.1093/infdis/jit547.